Figures and figure supplements

Atypical peripheral actin band formation via overactivation of RhoA and nonmuscle myosin II in mitofusin 2-deficient cells

Yueyang Wang *et al*.

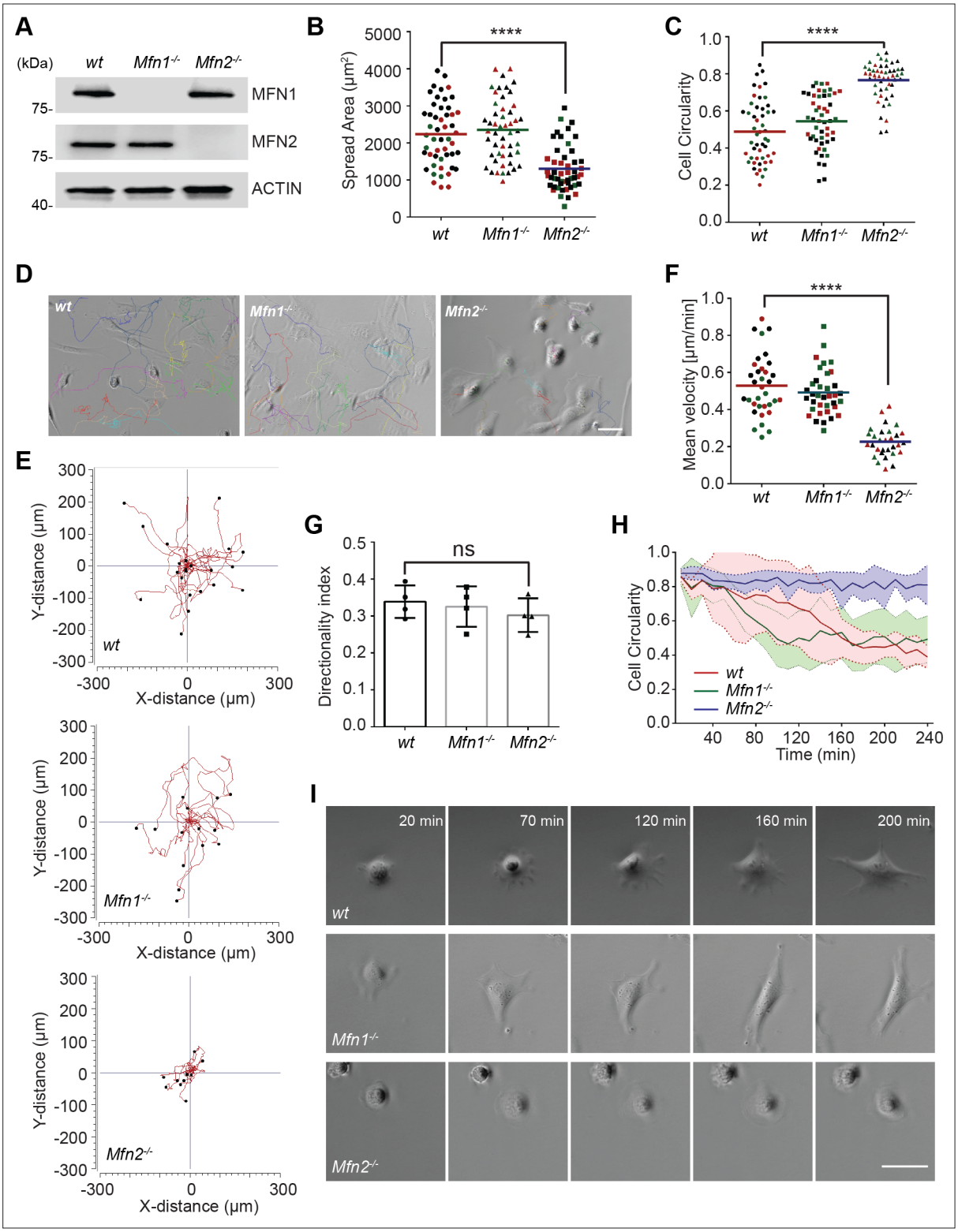

Figure 1. MFN2 regulates random migration and spreading in mice embryonic fibroblasts (MEFs). (**A**) Western blot determining the expression levels of MFN1 and MFN2 in wt, Mfn2-null, and Mfn1-null MEFs. (**B, C**) Spread area (**B**) and circularity (**C**) of wt, Mfn1-null, and Mfn2-null MEFs after overnight culture. The individual points represent individual MEF cells. (**D–G**) representative images with individual tracks (**D**), Wind–Rose plots (**E**), quantification of velocity (**F**), and directionality (**G**) of wt, Mfn1-null, and Mfn2-null MEFs cells during random migration. (**H, I**) Quantification of cell circularity (**H**) and representative images (**I**) of indicated MEFs during cell spreading at indicated time points. Data are presented as mean ± SD in (**F**) and were pooled from a total of 18 cells in three independent experiments. Bars represent arithmetic means ± SD. One representative result of three biological repeats is

Figure 1 continued on next page

Figure 1 continued

shown in (**A, D, E, I**). Data are pooled from three independent experiments in (**B, C, F, G**). n = 50 cells are tracked and counted in (**B, C**). N = 30 cells are quantified in (**D**). ****p<0.0001 (one-way ANOVA). Scale bars: 50 μm.

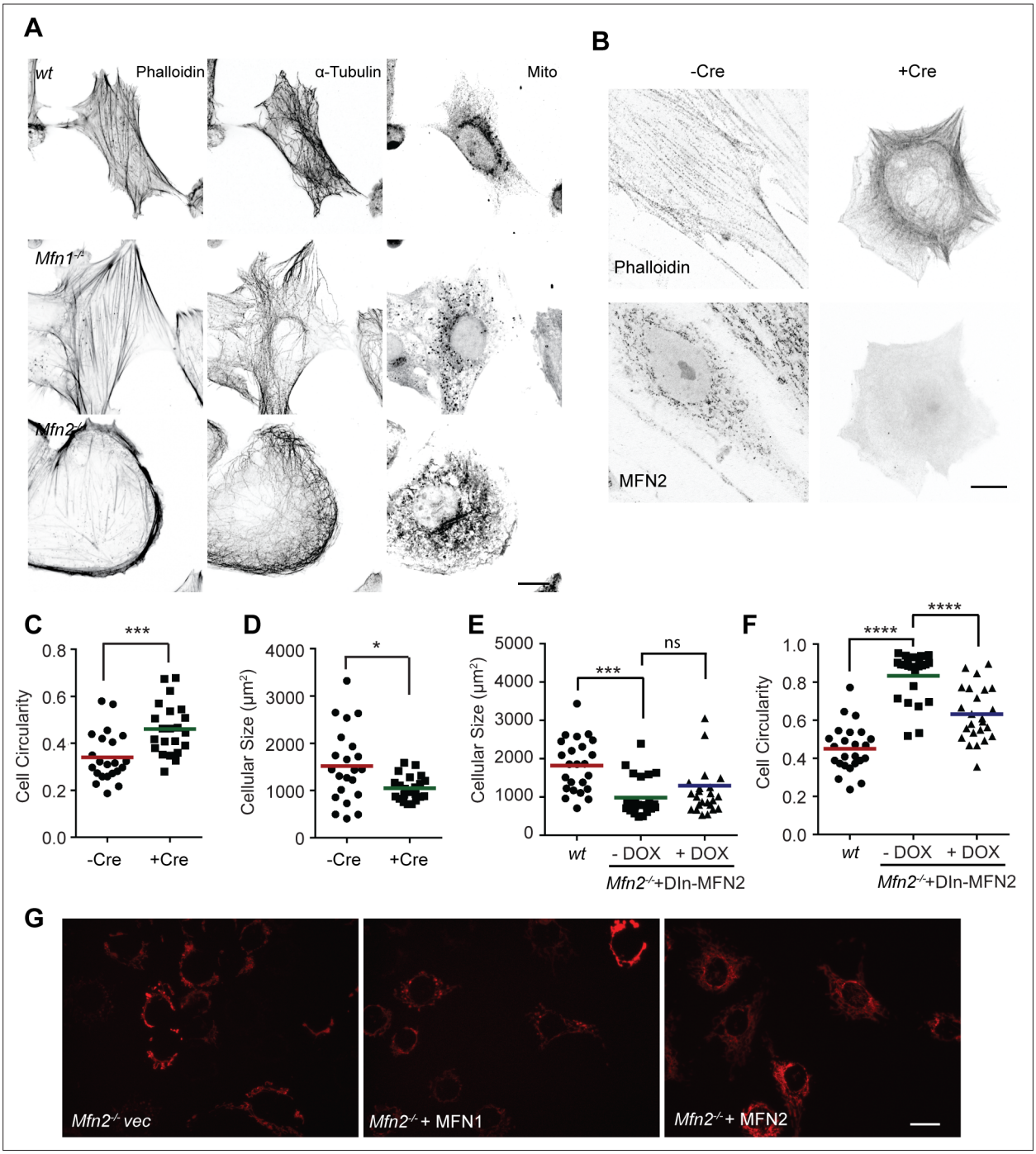

Figure 1—figure supplement 1. MFN2 deficiency changes mice embryonic fibroblast (MEF) morphology. (**A**) Immunofluorescence of F-actin (phalloidin), α-tubulin, and mitochondria (Mito Tracker) in *wt*, *Mfn1*-null, and *Mfn2*-null MEFs. (**B–D**) Cre-induced *Mfn2* disruption in MEFs from $Mfn2^{flox/flox}$ mice displays similar cell morphology as *Mfn2*-null MEFs (**B**). (**E, F**) Cell spread area (**E**) and circularity (**F**) of indicated cells in ***Figure 2J***. The individual points represent the circularity or spread area of individual MEF cells in (**C–F**). (**G**) Cells were transfected with mitochondria probes. *Mfn2*-null MEFs and *Mfn2*-null MEFs overexpressing MFN1 display large and fragmented mitochondria, while MFN2 re-expression in *Mfn2*-null MEFs restored mitochondria tubules. One representative result of three biological repeats is shown in (**A, B**). n = 25 cells in each group are quantified in (**C—F**). ***p≤0.001, ****p<0.0001 (one-way ANOVA). Scale bars: 10 μm in (**A, B**), 20 μm in (**G**).

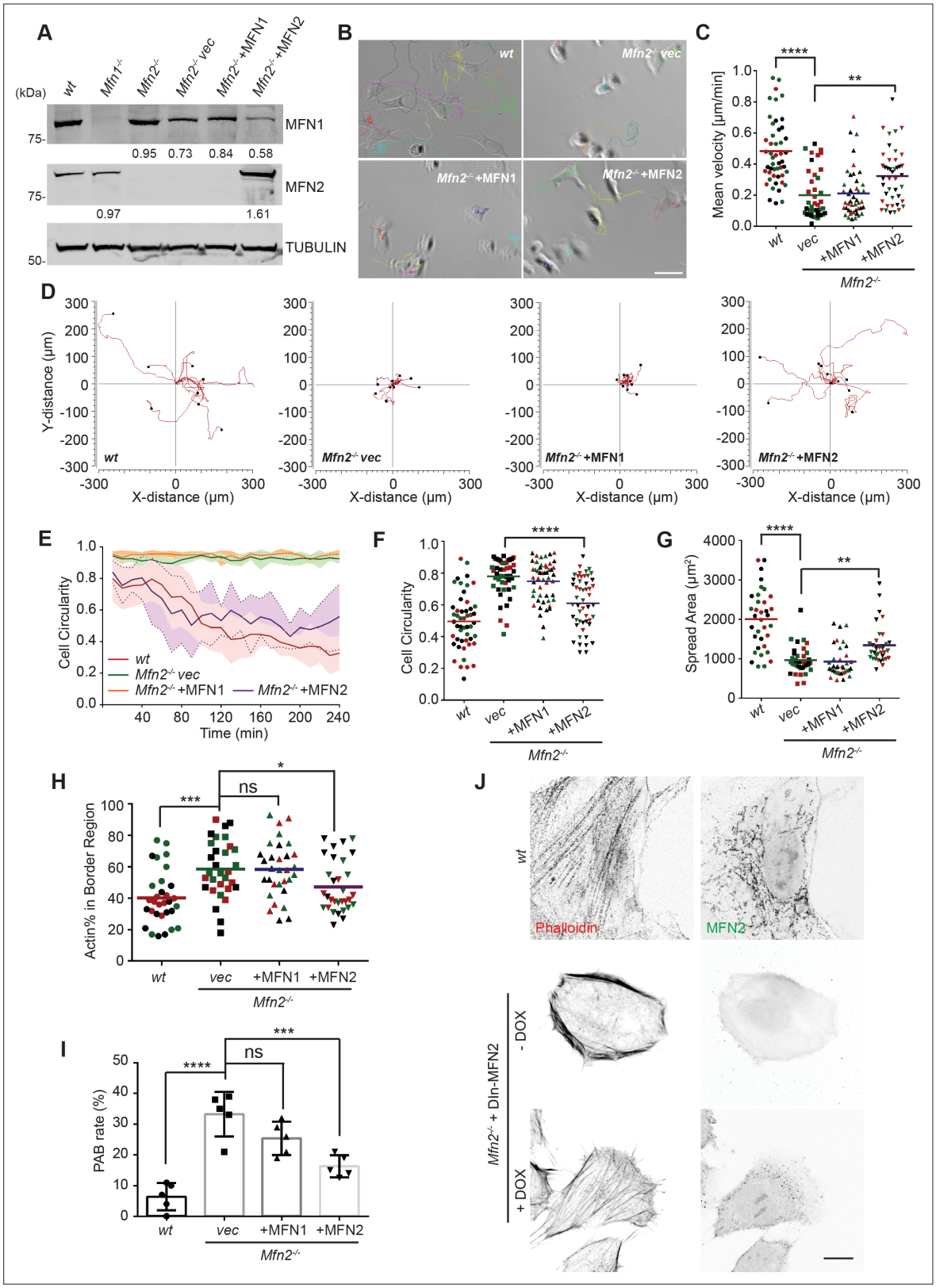

Figure 2. Cre expression of MFN2 rescues random migration and spreading defects in Mfn2-null mice embryonic fibroblasts (MEFs). (**A**) Western blot determining the expression level of MFN1 and MFN2 in indicated MEF cells. Percentages of knockdown or re-expression were calculated by normalizing the intensity to vinculin first, then normalizing to the wt group. (**B–D**) Representative images with individual tracks (**B**), quantification of velocity (**C**), and Wind–Rose plots (**D**) of indicated MEF cells during random migration. (**E**) Quantification of cell circularity of wt and Mfn2-null MEFs

Figure 2 continued on next page

Figure 2 continued

with vec, MFN1, or MFN2 re-expressed during spreading at indicated time points. Data are presented as mean ± SD in (**E**) (n = 5). (**F, G**) Cell circularity (**F**) and cell spreading area (**G**) of indicated MEFs measured after overnight culture. (**H, I**) Percentage of Actin abundance in the cell border region (**H**) and peripheral actin band (PAB) cell percentage in each view was quantified using our custom algorism (see ***Figure 2-figure supplement 1***). (**J**) Representative images of wt, Mfn2-null with doxycycline-induced MEF2 (DIn-MFN2) MEF cells treated with or without doxycycline for 48 hr. The cells are immunostained with phalloidin and MFN2. One representative result of three biological repeats is shown in (**A, B, D, H**). Data are pooled from three independent experiments in (**C, F–I**). n = 30 cells are tracked and counted in (**C**); n = 35 cells are quantified in (**F–H**). Five different views from three biological repeats are quantified in (**I**). *p≤0.05, **p≤0.01, ***p≤0.001, ****p<0.0001 (one-way ANOVA in **C, E, F**, unpaired *t*-test in **H, I**). Scale bars: 50 μm in (**B**), 10 μm in (**J**).

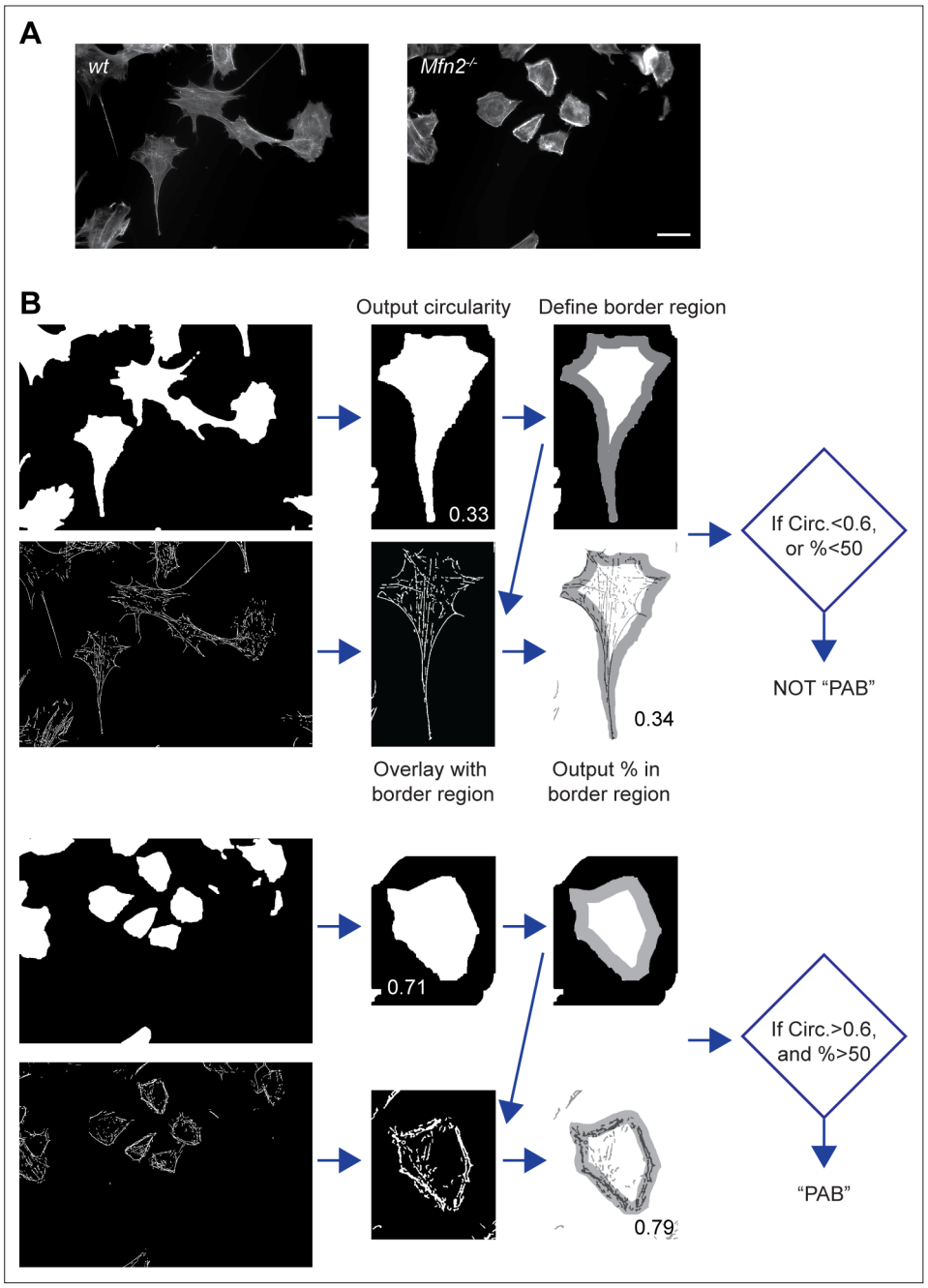

Figure 2—figure supplement 1. Custom algorithm to identify cells with peripheral actin band (PAB). (**A**) Representative images of *wt* and *Mfn2*-null mice embryonic fibroblasts (MEFs) stained with F-actin (phalloidin) under a 40× microscope. Scale bar: 50 μm. (**B**) FiloQuant plugin in ImageJ was used to identify cell edges and the actin cytoskeleton. The algorithm defines a 20-pixel stroke inside the cell border as the 'border region' and then calculates the percentage of the actin cytoskeleton in the border region and the cell circularity. If the circularity is higher than 0.6, and more than 50% of the actin cytoskeleton is in the border region, we consider the cell a PAB cell.

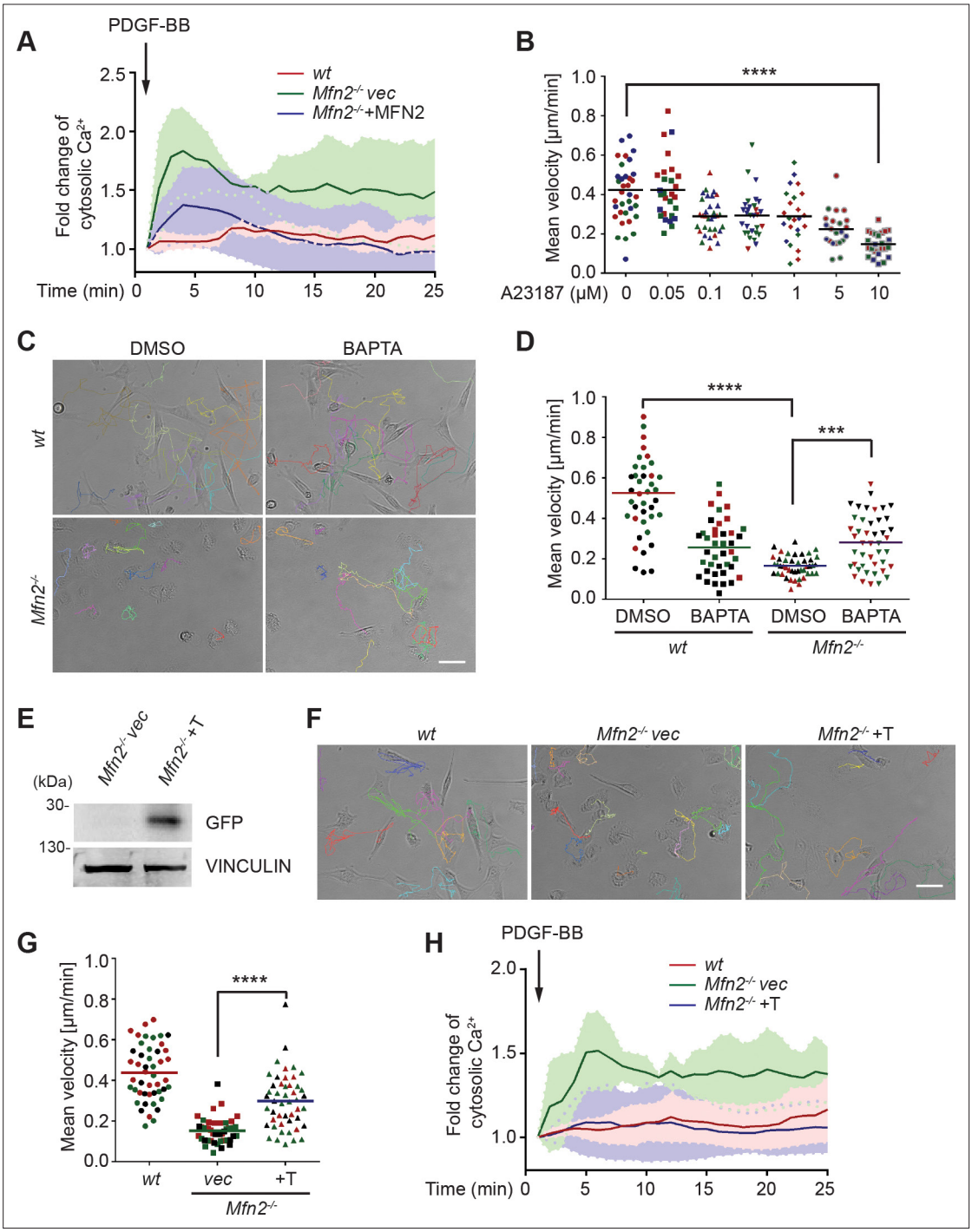

Figure 3. CMFN2 regulates random migration through cytosolic Ca^{2+} and endoplasmic reticulum (ER)-mitochondria tether. (**A**) Fluo-4 recordings of cytosolic Ca^{2+} in the indicated cell lines after PDGF-BB stimulation. (**B**) Quantification of the velocity of *wt* mice embryonic fibroblast (MEF) random migration in the presence of vehicle or different concentrations of the Ca^{2+} ionophore A23187. (**C, D**) Representative images with individual tracks (**C**) and quantification of velocity (**D**) of wt or Mfn2-null MEFs during random migration with or without the presence of the intracellular calcium chelator BAPTA-AM. (**E**) Western blot of GFP in indicated cell lines. $Mfn2^{-/-}$+T, Mfn2-null MEFs with synthetic ER-GFP-mitochondria tether construct. (**F, G**) Representative images with individual tracks (**F**) and quantification of velocity (**G**) of indicated MEF cells. (**H**) Fluo-4 recordings of cytosolic Ca^{2+} in the indicated cell lines after PDGF-BB stimulation. The individual points in (**B, D, G**) are the mean speeds for individual MEF cells. Data are presented as mean ± SD in (**A, H**). Data are pooled from three independent experiments in (**A, H**). One representative result of three biological repeats is shown in (**C–G**). n = 30 cells are tracked and counted in (**B, G**). n = 35 cells are tracked and measured in (**D**). ***p<0.001, ****p<0.0001 (one-way ANOVA in **B, G** and two-way ANOVA in **D**). Scale bars: 50 μm.

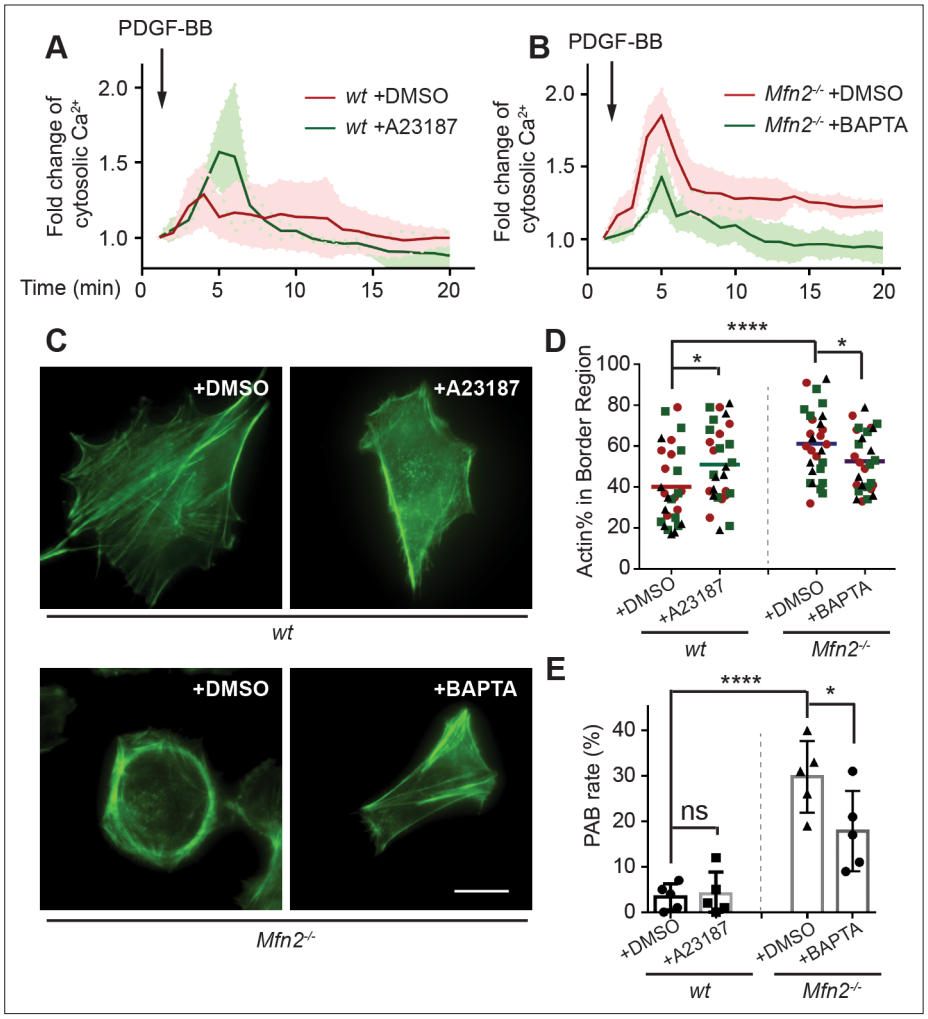

Figure 3—figure supplement 1. Excessive cytosolic Ca^{2+} is insufficient to phenocopy the peripheral actin band ('PAB') structure in *wt* mice embryonic fibroblasts (MEFs), while the cytosolic Ca^{2+} inhibitor BAPTA rescues 'PAB' structure in *Mfn2*-null MEFs. (**A, B**) Fluo-4 recordings of cytosolic Ca^{2+} in the indicated cell lines after PDGF-BB stimulation. (**C**) Immunofluorescence of F-actin (phalloidin) in wt MEFs treated with DMSO or A23187, and *Mfn2*-null MEFs treated with DMSO or BAPTA. (**D, E**) Percentage of actin abundance in the cell border region (**D**) and the percentage of PAB cells (**E**) identified by our custom algorism in indicated cell lines. Data are pooled from three independent experiments and presented as mean ± SD in (**A, B**). n = 28 cells are measured in (**D**). Five different views from two biological repeats are quantified in (**E**). *p≤0.1, ****p<0.0001 (two-way ANOVA in **D, E**). Scale bars: 20 μm.

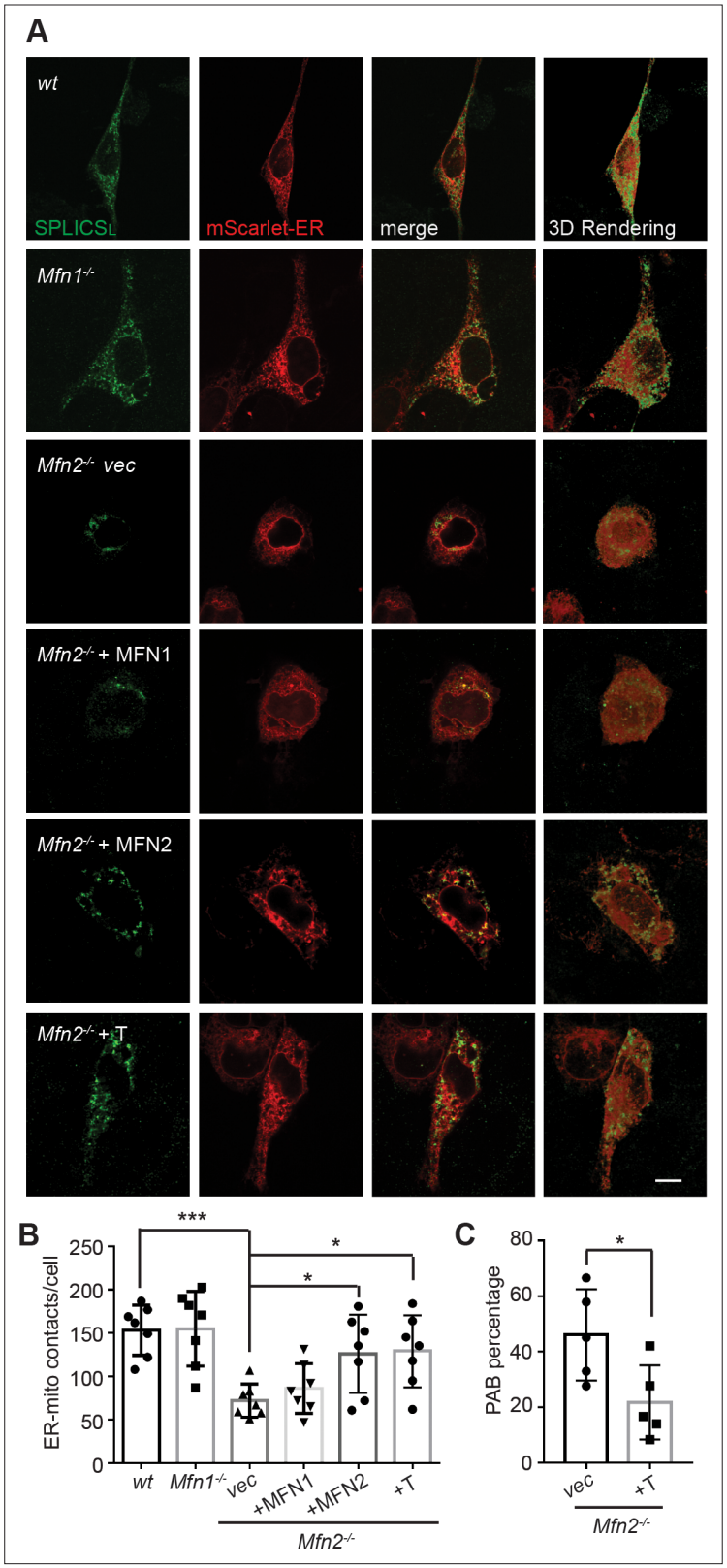

Figure 3—figure supplement 2. Expression of MEF2 or an endoplasmic reticulum (ER)-mitochondria tether construct restores ER-mitochondria contacts and mitochondria morphology. (**A, B**) Cells were co-transfected with the ER probe and SPLICS$_L$ Mt-ER long P2A probe. Representative images of SPLICS$_L$ probe (green) and ER (red) (**A**) and quantification (**B**) of SPLICS$_L$ contacts by 3D rendering of complete z-stacks. (**C**) Peripheral actin band (PAB)

Figure 3—figure supplement 2 continued on next page

Figure 3—figure supplement 2 continued

cell percentage was quantified using our custom algorithm in *Mfn2*-null mice embryonic fibroblasts (MEFs) with *vec* or ER-mito tethering construct. n = 7 cells from two independent experiments. Five different views from two biological repeats are quantified in (**C**). *p≤0.1, ***p≤0.001 (one-way ANOVA in **B**, Student's *t*-test in **C**). Scale bars: 20 μm.

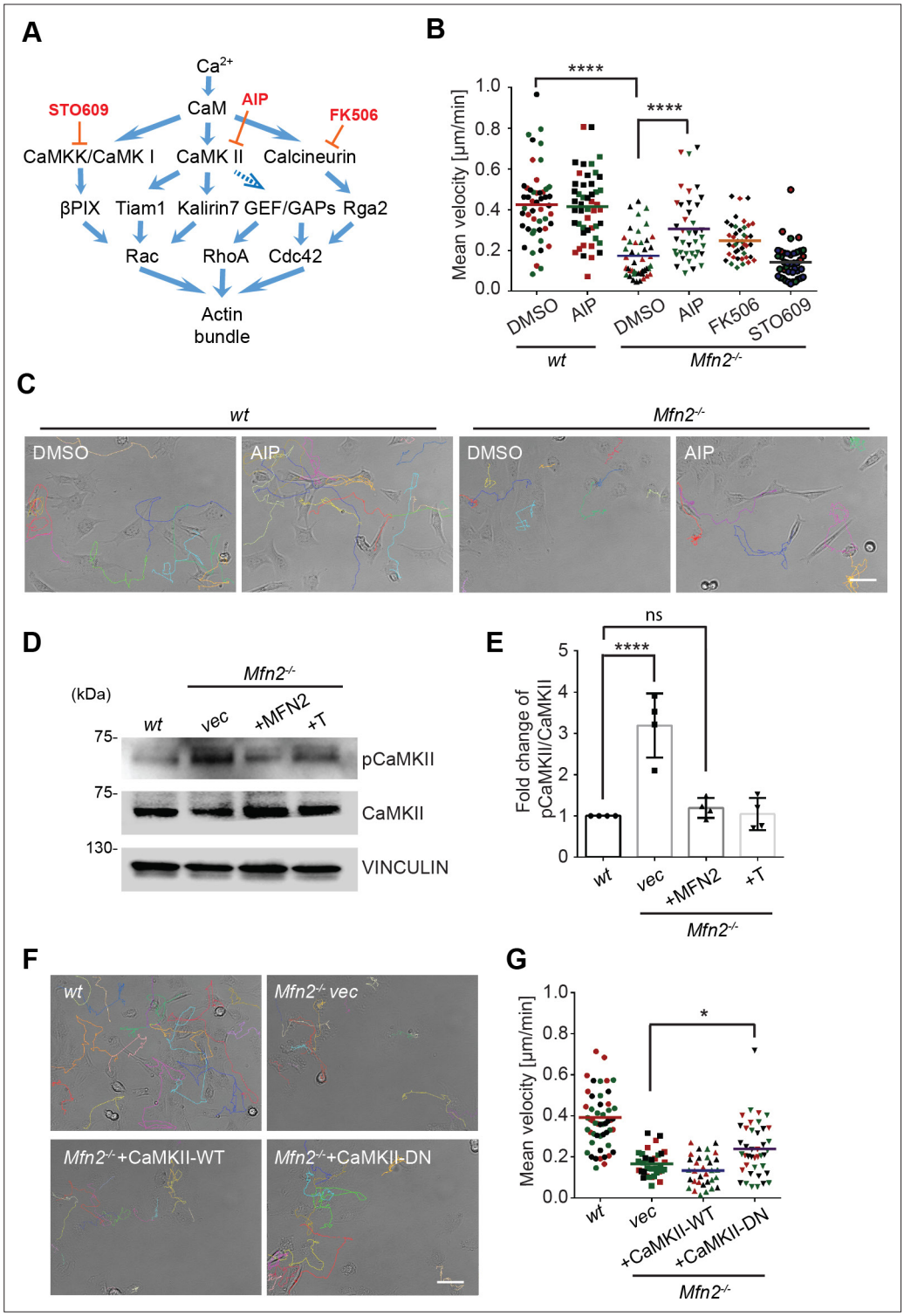

Figure 4. CaMKII activation mediates Mfn2 deficiency-induced inhibition in mice embryonic fibroblast (MEF) migration. (**A**) Selected signaling cascades involved in the regulation of the actin cytoskeleton via Ca^{2+}. Blue arrows indicate positive regulation. Dashed blue arrows indicate positive regulation with unclear mechanisms. Orange T-shaped bars indicate negative regulation of the pharmacological inhibitors. (**B**) Quantification of the velocity of indicated MEF cells treated with DMSO, the CaMKII inhibitor AIP, the Calcineurin inhibitor FK506, or the CaMKK inhibitor STO609. (**C**) Representative images with individual tracks of wt or Mfn2-null MEFs treated with the CaMKII inhibitor AIP. (**D, E**) Western blot (**E**) and quantification (**F**) determining the amount of pCaMKII and pan-CaMKII in wt, Mfn2-null MEFs with vec, CaMKII-WT, or CaMKII-DN overexpressed after treating with 25 μM PDGF-BB for

Figure 4 continued on next page

Figure 4 continued

4 min. (**F, G**) Quantification of velocity (**G**) and representative images with individual tracks (**F**) of wt, Mfn2-null MEFs with vec, CaMKII-WT, or CaMKII-DN overexpressed during random migration. One representative result of three biological repeats is shown in (**B, C, F, G**). Four biological repeats are shown in (**E**). n = 40 cells are quantified in (**B, G**). *p≤0.05, ***p≤0.001, ****p<0.0001 (one-way ANOVA in **E, G** and two-way ANOVA in **B**). Scale bars: 50 μm.

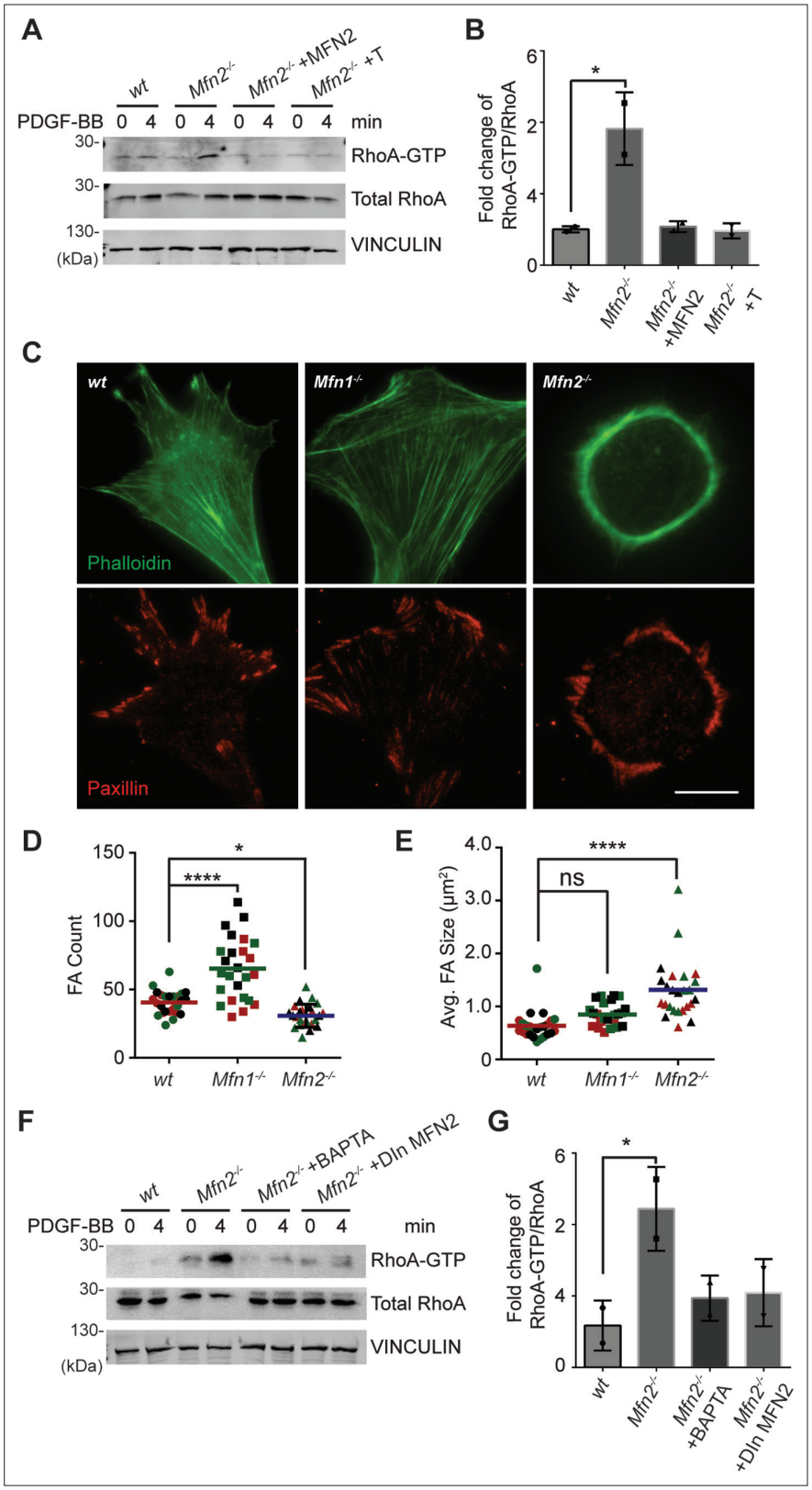

Figure 5. Loss of MFN2 induces heightened RhoA activation in mice embryonic fibroblasts (MEFs). (**A, B**) RhoA pulldown activation assay demonstrates increased RhoA-GTP in *Mfn2*-null MEFs, which can be corrected by re-expressing MFN2 or inducing a mitochondria-endoplasmic reticulum (ER) tether. (**A**) Western blot and (**B**) quantification determining the amount of RhoA-GTP and total RhoA protein in *wt*, *Mfn2*-null MEFs, *Mfn2*-null

Figure 5 continued on next page

Figure 5 continued

MEFs with MFN2 re-expression, or with an artificial ER-mitochondria tether; the indicated cell lines were treated with 25 ng/ml PDGF-BB for 0 or 4 min. (**C**) Immunofluorescence of F-actin (phalloidin) and Paxillin in *wt*, *Mfn1*-null, and *Mfn2*-null MEFs after overnight culture. (**D, E**) *Mfn2*-null MEFs display slightly decreased FA numbers (**D**) but significantly larger FA sizes (**E**). (**F, G**) RhoA pulldown activation assay demonstrates cytosolic Ca^{2+} inhibition corrects RhoA-GTP level in *Mfn2*-null MEFs. (**F**) Western blot and (**G**) quantification showing the amount of RhoA-GTP protein in *wt*, *Mfn2*-null MEFs, *Mfn2*-null MEFs treated with BAPTA, or *Mfn2*-null MEFs with doxycycline (DOX)-induced MFN2 re-expression for 48 hr; the indicated cells were treated with 25 ng/ml PDGF-BB for the indicated time. RhoA-GTP/total RhoA ratios at 4 min were normalized to 0 min to show the fold changes in (**B, G**). n = 30 cells were quantified in (**D, E**). One representative result of two biological repeats is shown in (**A, B, F, G**). *p≤0.05 (one-way ANOVA comparing each group with the average of the *wt* group). Scale bar: 50 μm.

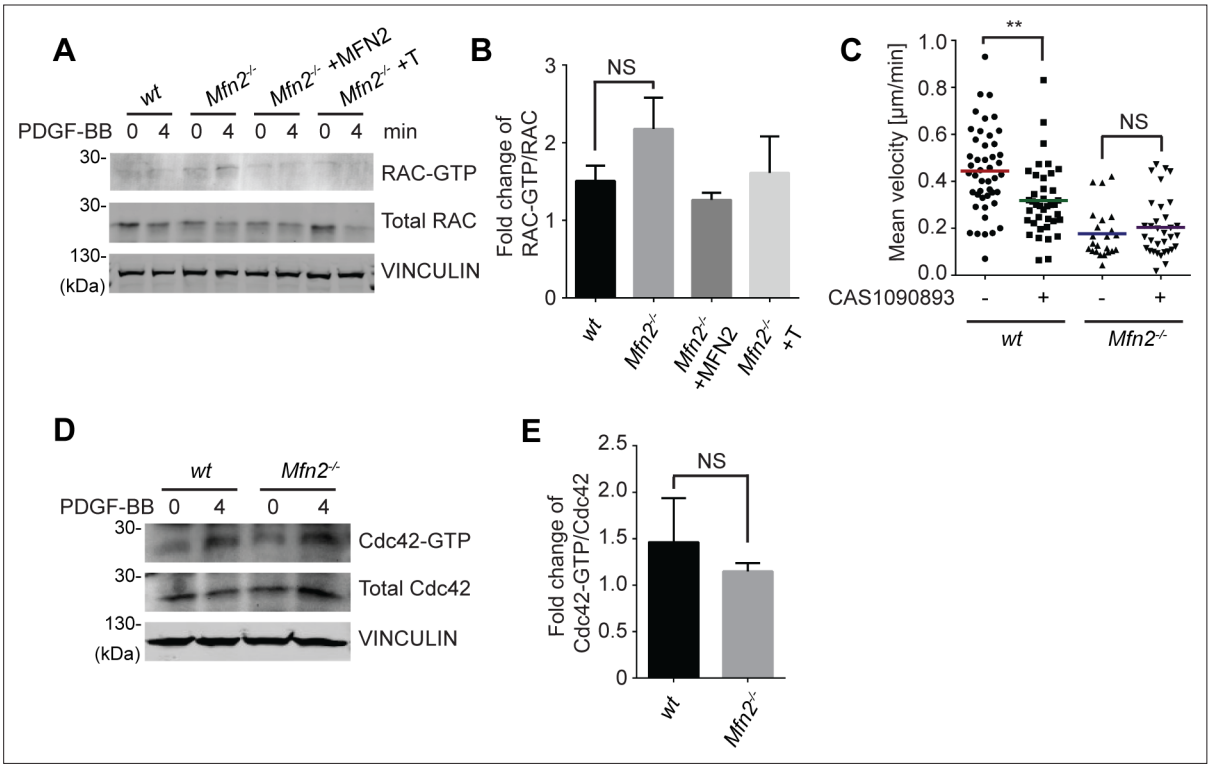

Figure 5—figure supplement 1. Activities of Rac and Cdc42 are not increased in MFN2-deficient mice embryonic fibroblasts (MEFs). (**A**) Western blot and (**B**) quantification of the amount of RAC-GTP and total RAC protein in wt, Mfn2-null MEFs, Mfn2-null MEFs with MFN2 re-expressed, or with an artificial endoplasmic reticulum (ER)-mitochondria tether. The indicated cell lines were treated with 25 ng/ml PDGF-BB for 0 or 4 min. (**C**) Quantification of the velocity of indicated MEF cells treated with DMSO or Rac inhibitor CAS1090893 (50 μM) overnight. (**D, E**) Cdc42 pulldown activation assay demonstrates no difference in Cdc42-GTP in wt and Mfn2-null MEFs. (**D**) Western blot and (**E**) quantification of the amount of CDC42-GTP and total CDC42 protein in wt, Mfn2-null MEFs treated with 25 ng/ml PDGF-BB 0 or 4 min. One representative result of three biological repeats is shown in (**A, D**). Data are pooled from three independent experiments in (**B, C, E**). n > 25 cells were quantified in **C**. Error bars represent SD. NS, nonsignificant (two-way ANOVA in **C**, one-way ANOVA in **B**, unpaired *t*-test in **E**).

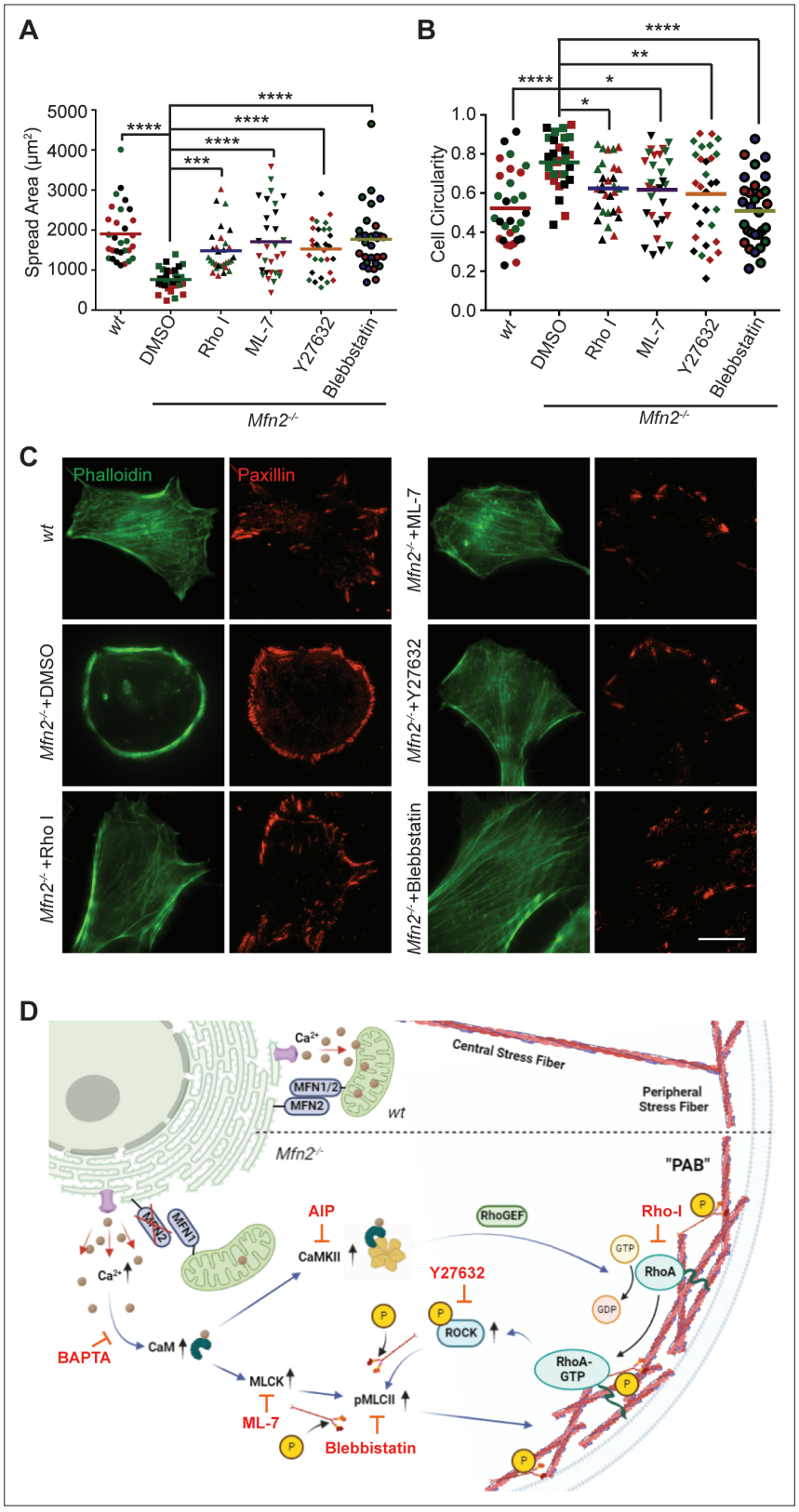

Figure 6. Small-molecule inhibitors targeting RhoA- and MLCK-related signaling pathways rescue MFN2 deficiency-induced phenotypes. (**A, B**) Cellular spread area (**A**) and circularity (**B**) of *wt* and *Mfn2*-null mice embryonic fibroblasts (MEFs) treated with indicated inhibitors overnight. (**C**) Immunofluorescence of F-actin (phalloidin) and Paxillin in *wt* and *Mfn2*-null MEFs treated with indicated inhibitors overnight. (**D**) Schematic of

Figure 6 continued on next page

Figure 6 continued

the effectors and their inhibitors (red) in MFN2-regulated signaling network leading to Actin bundle. Increased cytosolic Ca^{2+} may activate MLCK, CaMKII, and RhoA-ROCK, which activate MLC and affect actin bundle formation. One representative result of three biological repeats is shown in (**C**). Data are pooled from three independent experiments, and n = 30 cells are quantified in (**A, B**). *p≤0.05, **p≤0.01, ***p≤0.001, ****p<0.0001 (one-way ANOVA comparing each group to the average of *Mfn2*$^{-/-}$ DMSO group). Scale bars: 50 μm.

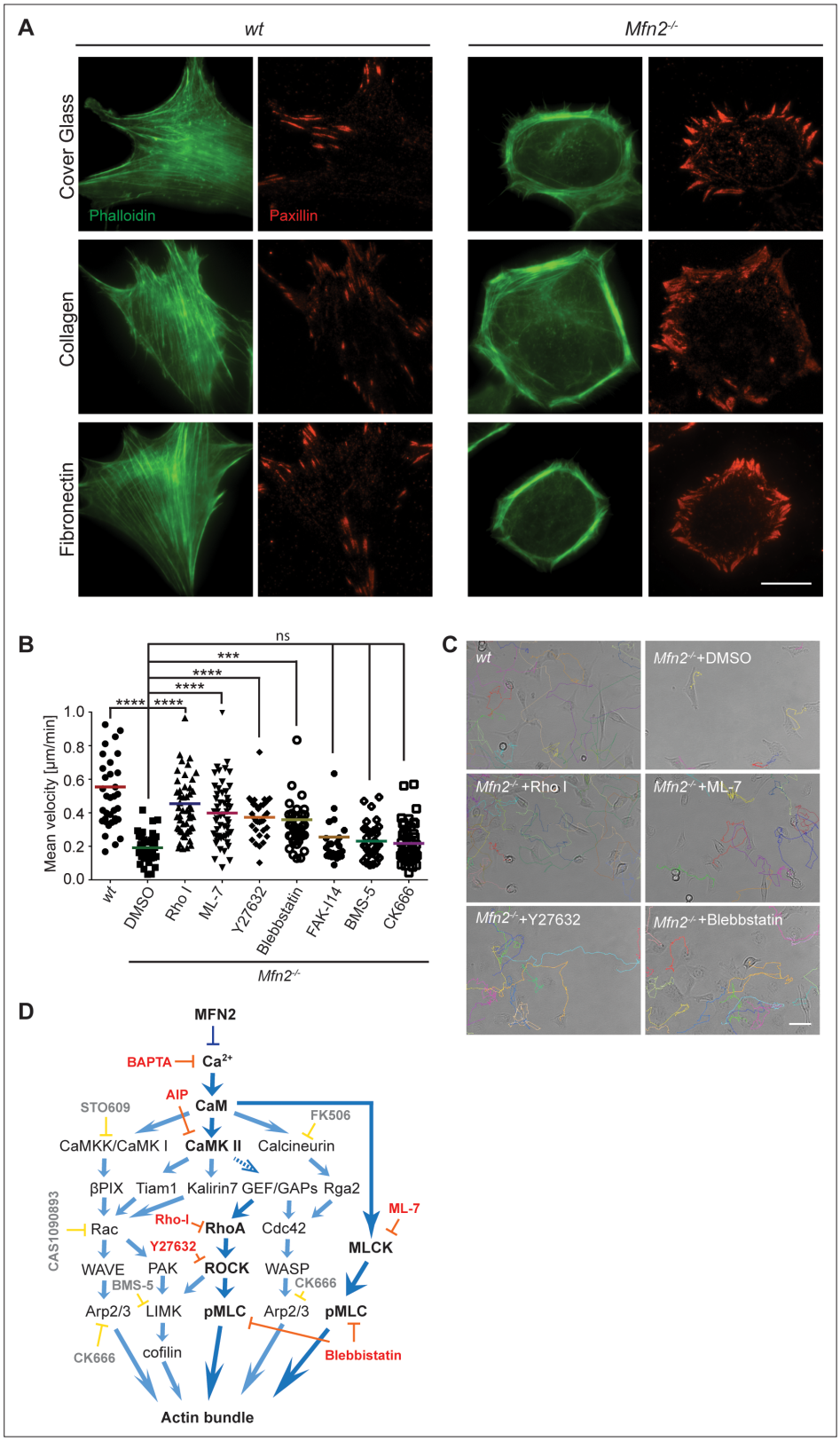

Figure 6—figure supplement 1. RhoA and MLC drive peripheral actin band ('PAB') structure in MFN2-deficient mice embryonic fibroblasts (MEFs). (**A**) Immunofluorescence of F-actin (phalloidin) and Paxillin in *wt* and *Mfn2*-null MEFs cultured on uncoated, collagen-coated, or fibrinogen-coated cover glasses. (**B**) Velocity quantification of indicated MEF cells treated with DMSO, the Rho inhibitor-I, the MLCK inhibitor ML-7, the ROCK inhibitor

Figure 6—figure supplement 1 continued on next page

Figure 6—figure supplement 1 continued

Y27632, the myosin inhibitor Blebbistatin, FAK inhibitor-14, the LIM kinase inhibitor BMS-5, or the Arp2/3 inhibitor CK666. (**C**) Representative images with individual tracks of indicated MEF cells treated with DMSO or indicated inhibitors. (**D**) A small-molecular inhibitor screen revealed the schematic of the effectors and their inhibitors (red) in the MFN2-regulated signaling network leading to the Actin bundle. Data are pooled from three independent experiments in (**B**) and n>30 cells are quantified. ***p≤0.001, ****p<0.0001 (one-way ANOVA comparing each group to the average of *Mfn2*$^{-/-}$ DMSO group). Scale bars: 50 μm.

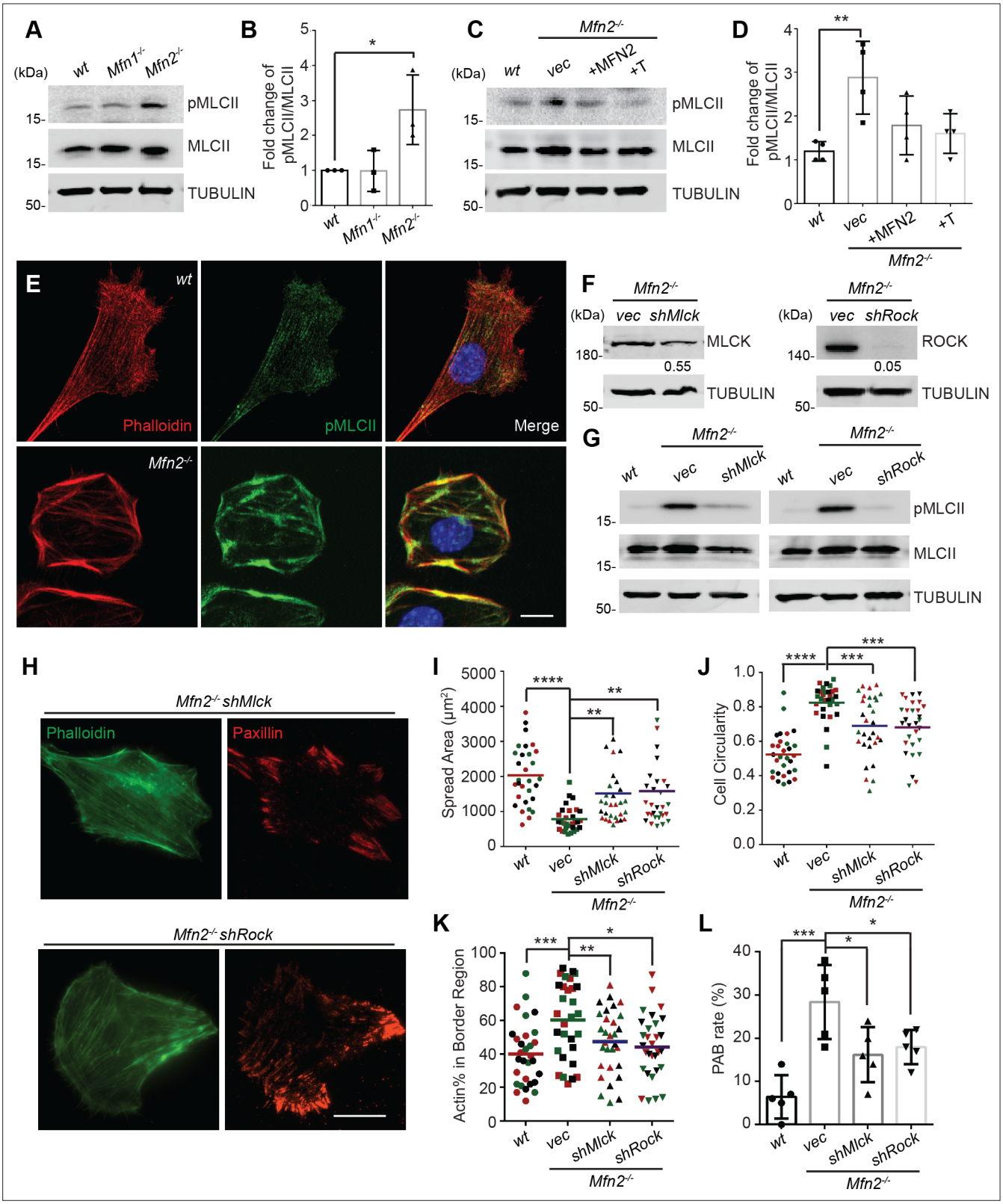

Figure 7. Heightened MLC activity promotes the peripheral actin band ('PAB') structure in MFN2-deficient mice embryonic fibroblasts (MEFs). (**A, B**) Western blot (**A**) and quantification (**B**) of the amount of pMLCII and total MLCII in *wt*, *Mfn1*-null, and *Mfn2*-null MEFs. (**C, D**) Increased pMLCII in *Mfn2*-null MEFs can be corrected by re-expressing MFN2 or inducing a mitochondria-endoplasmic reticulum (ER) tether. (**C**) Western blot and (**D**) quantification determining the amount of pMLCII and total MLCII protein in *wt*, *Mfn2*-null MEFs, *Mfn2*-null MEFs with MFN2 re-expressed, or with

Figure 7 continued on next page

Figure 7 continued

an artificial ER-mitochondria tether. (**E**) Representative images of *wt* and *Mfn2*-null MEFs immunostained for F-actin (phalloidin), pMLCII, and DAPI. (**F**) Western blot determining the expression levels of MLCK or ROCK in *Mfn2*-null MEFs with *shMLCK* or *shROCK*. (**G**) Western blot of pMLCII and total MLCII *Mfn2*-null MEFs with *shMLCK* or *shROCK*. (**H**) Representative images of *Mfn2*-null MEFs with *shMLCK* or *shROCK* immunostained for F-actin (green) and paxillin (red). (**I, J**) Cellular spread area and circularity of *wt*, *Mfn2*-null MEFs with *vec, shMLCK,* or *shROCK* were measured after overnight culture. (**K**) Percentage of actin abundance in the cell border region in *wt*, *Mfn2*-null MEFs, *Mfn2*-null MEFs with *shMLCK* or *shROCK*. (**L**) Percentage of PAB cells identified by a custom algorithm in *wt*, *Mfn2*-null MEFs, *Mfn2*-null MEFs with *shMLCK* or *shROCK*. The individual points stand for the size or circularity of individual MEF cells. One representative result of three biological repeats is shown in (**A, B, F, G**). Four biological repeats were done in (**C, D**). Data are pooled from three independent experiments in (**I, J**). n = 30 cells are quantified in (**I, K**). Five different views from three biological repeats are quantified in (**L**). *p≤0.05, **p≤0.01, ***p≤0.001, ****p<0.0001 (one-way ANOVA, comparing each group to the average of $Mfn2^{-/-}$ *vec* group in **I, K**). Scale bars: 20 μm in (**H**), 10 μm in (**E**).

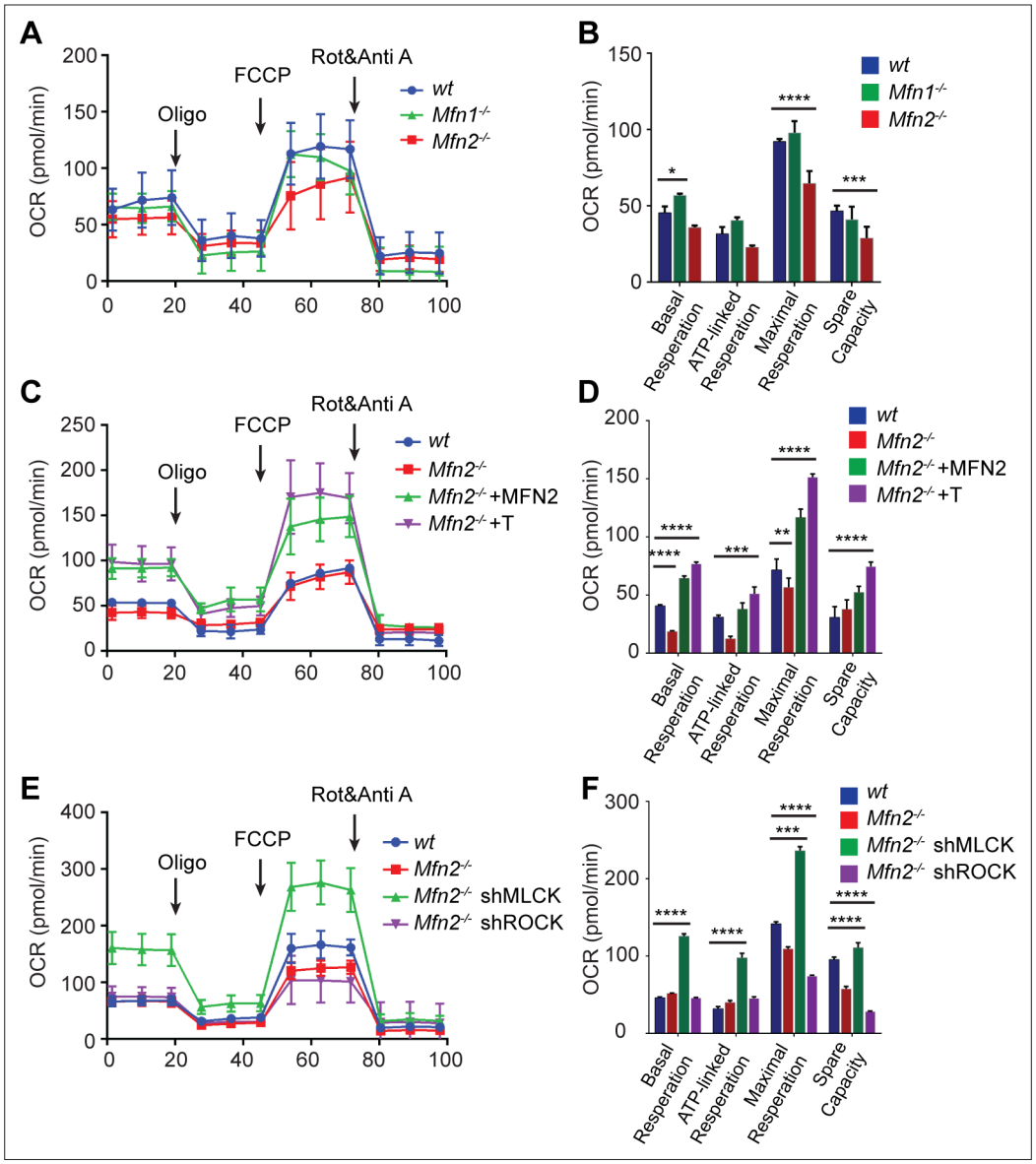

Figure 7—figure supplement 1. The cell lines with restored motility show different oxygen consumption rates. (**A, C, E**) Representative graph showing oxygen consumption rate (OCR) of indicated mice embryonic fibroblast (MEF) cells. (**B, D, F**) Basal respiration, ATP-linked respiration, maximal respiratory, and spare capacity of indicated cell lines. One representative result of three biological repeats in (**A–F**). Error bars represent SD. *p≤0.05, **p≤0.01, ***p≤0.001, ****p<0.0001 (two-way ANOVA).

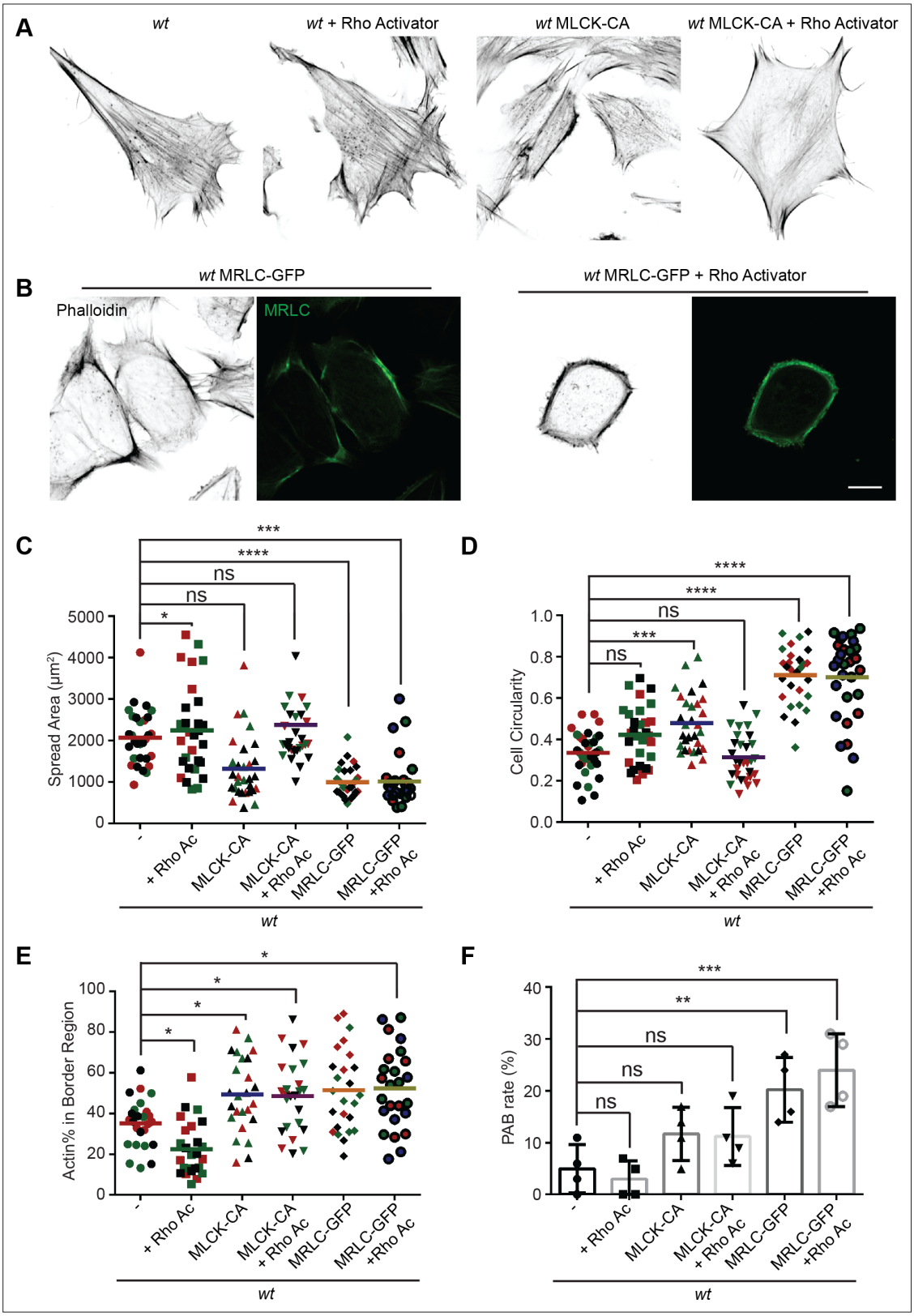

Figure 8. MRLC overexpression and Rho activation in *wt* mice embryonic fibroblasts (MEFs) recapitulates the peripheral actin band ('PAB') structure. (**A**) Immunofluorescence of F-actin (phalloidin) in *wt* MEFs with or Rho activator treatment or introducing MLCK-CA expression. (**B**) Representative images of *wt* MEFs expressing MRLC-GFP with or without the Rho Activator, immunostained for F-actin (phalloidin). (**C, D**) Spread area and circularity of *wt* MEFs with the indicated overexpression or drug treatment. The individual points stand for the size or circularity of individual MEF cells. (**E,**

Figure 8 continued on next page

Figure 8 continued

F) Percentage of actin abundance in the cell border region (**E**) and the percentage of PAB cells (**F**) identified by our custom algorism in indicated cell lines. One representative result of three biological repeats is shown in (**A, B**). Data are pooled from three independent experiments in (**C–E**). n = 30 cells are tracked and counted in (**C–E**). Four different views from three biological repeats are quantified in (**F**). *p≤0.05, **p≤0.01, ***p≤0.001, ****p<0.0001 (one-way ANOVA, comparing each column with the mean of the *wt* group). Scale bars: 10 μm.

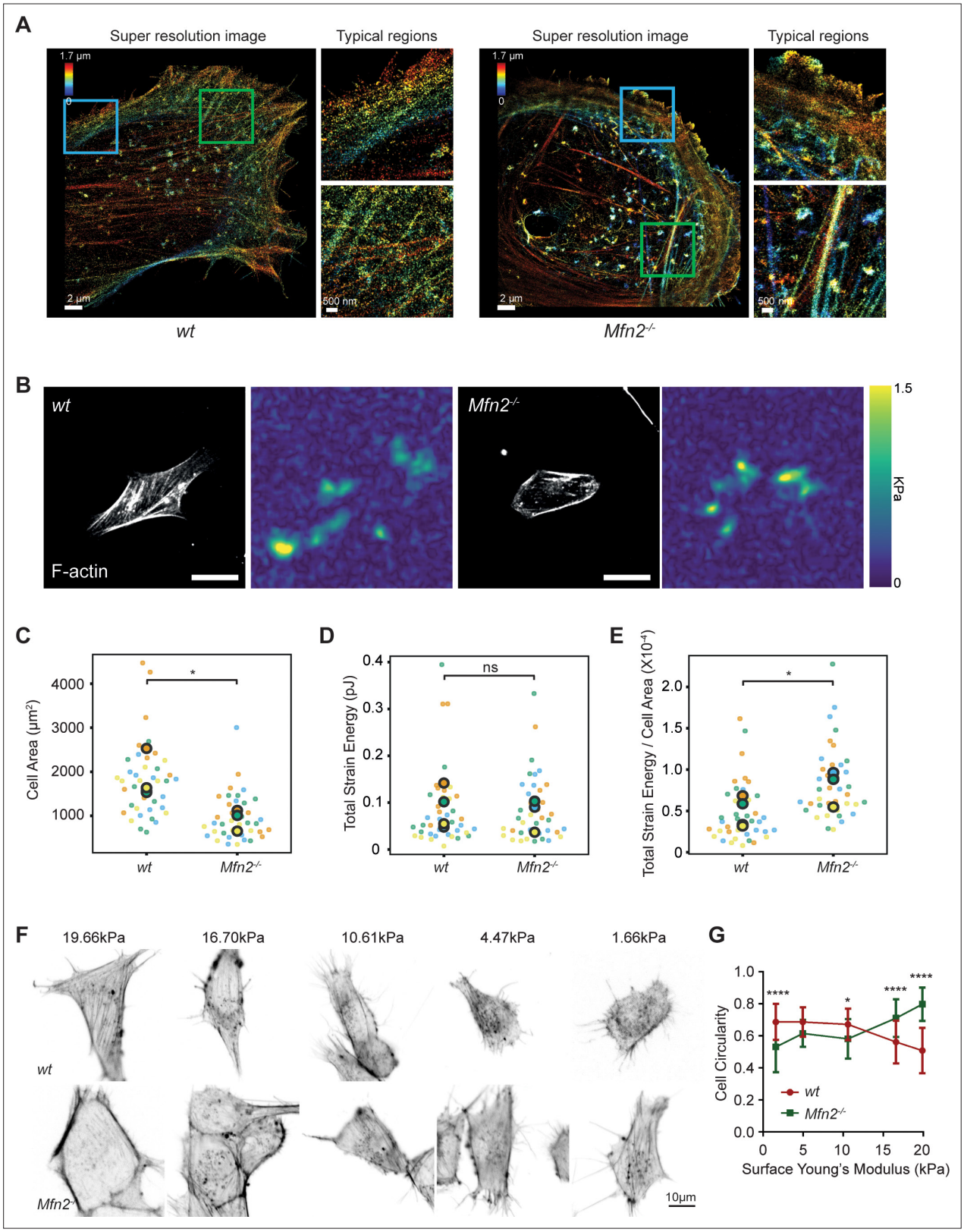

Figure 9. Mfn2-null mice embryonic fibroblasts (MEFs) exhibit altered actin organization and cell stiffness. (**A**) 3D super-resolution reconstructions of immunofluorescence-labeled F-actin in wt or Mfn2-null MEFs. x–y overview of a 1.7-μm-thick volume of the cells. (**B**) Morphology of indicated MEF cells on polyacrylamide (PAA) substrates after overnight culture immunostained with Alexa-488 phalloidin. A traction stress map with color values corresponding to different stress values is shown on the right. Scale bars: 50 μm. Quantification of the corresponding cell spreading areas (**C**), total

Figure 9 continued on next page

Figure 9 continued

strain energy (**D**), and total strain energy normalized to cell area (**E**). (**F**) Representative images of indicated MEF cells on polyacrylamide (PAA) substrates of different stiffness after overnight culture. The cells are immunostained with Alexa-488 phalloidin. (**G**) The cell circularity of the indicated cells is measured. The individual points stand for the circularity of individual MEF cells. One representative result of three biological repeats is shown in (**C, F**). Data are pooled from three independent experiments in (**C–E, G**). n > 40 cells are counted in (**B–E**). *p≤0.05, ****p<0.0001 (unpaired *t*-test). Scale bars: 2 μm in (**A**), 50 μm in (**B**), and 10 μm in (**F**).

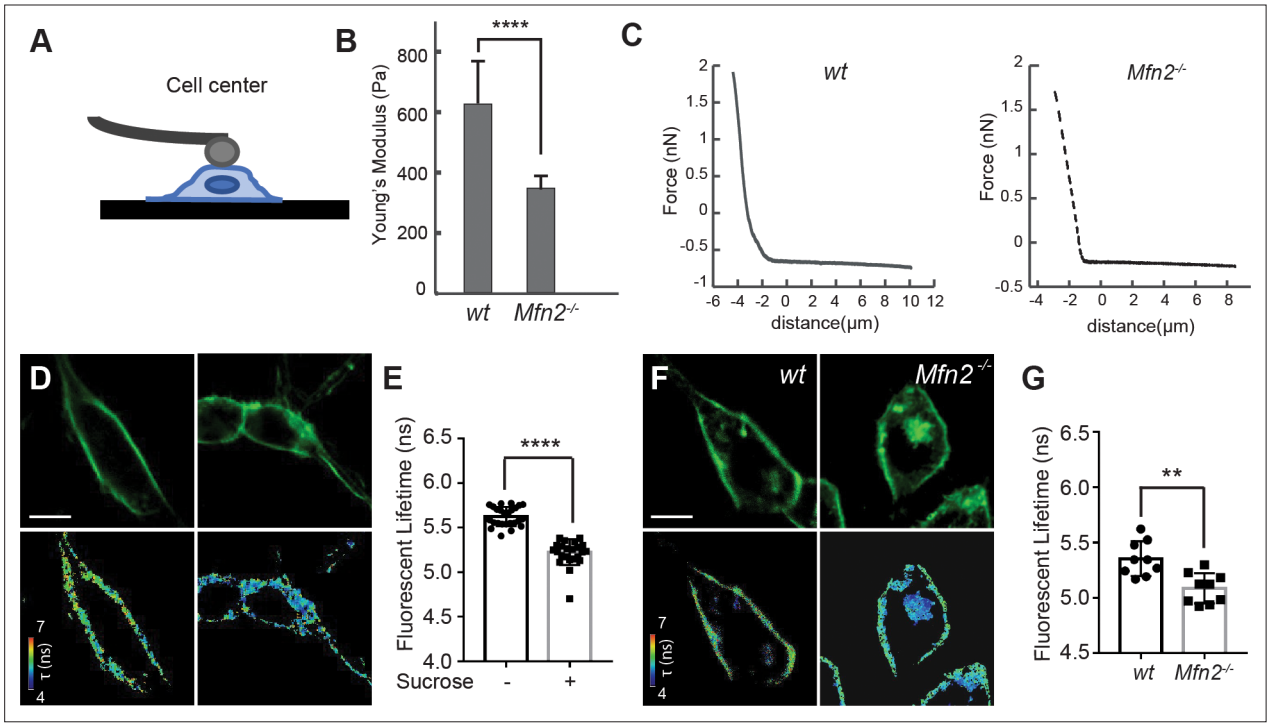

Figure 9—figure supplement 1. *Mfn2*-null mice embryonic fibroblasts (MEFs) exhibit altered cell stiffness and membrane tension. (**A**) Schematic of the cantilever probe indenting cells at cell center during atomic force microscopy (AFM) process. (**B**) Measurement of effective cell modulus (mean ± SEM) of *wt* or *Mfn2*-null MEFs (n ≥ 15 for each group). (**C**) Representative AFM force curves of the cantilever probe *wt* or *Mfn2*-null MEFs. (**D**) Representative FLIM images and (**E**) quantification of the Flipper-TR probe's lifetime on wt MEFs under regular and hypertonic conditions. (**F**) Representative FLIM images and (**G**) quantification of the Flipper-TR probe's lifetime on *wt* and *Mfn2*-null MEFs. One representative result of three biological repeats in (**A, D, F**). Data are pooled from three independent experiments in (**B**). Error bars represent SD. **p≤0.01, ****p<0.0001 (unpaired *t*-test in **B, E, G**).